THE BALTIC JOURNAL
OF ROAD AND BRIDGE ENGINEERING

ISSN 1822-427X / eISSN 1822-4288
2016 Volume 11(2): 102–110

IMPACT OF TRAIN-INDUCED VIBRATION ON RAILWAY CABLE-STAYED BRIDGES FATIGUE EVALUATION

Shiling Pei[1], Yongle Li[2]✉, Yulong Bao[3], Xin Li[4], Shizhong Qiang[5]

[1]*Colorado School of Mines, Golden CO 80401, U.S.A,*
[2, 5]*Dept of Bridge Engineering, Southwest Jiaotong University, Chengdu 610031, P. R. China*
[3]*Key Laboratory of Large–span Bridge Construction Technology, Wuhan 430048, P. R. China*
[4]*MOE Key Laboratory of High Speed Railway Engineering, Southwest Jiaotong University, Chengdu 610031, P. R. China*
E–mails: [1]*spei@mines.edu ;* [2]*lele@swjtu.edu.cn;* [3]*baoyulong1991@my.swjtu.edu.cn;* [4]*shectc@sneb.com.cn;*
[5]*qiangshizhong@163.com*

Abstract. Under repetitive heavy train traffic, railway steel truss bridges tend to have many fatigue related performance issues, especially at welded joints. Accurate estimation of the stress history at critical locations of welded joints under vehicle loading is important for joint fatigue design. Traditionally, vehicle loads were treated as moving static loads without considering their dynamic effects. In this study, a numerical procedure was introduced to incorporate the effect of dynamic response of the train–bridge coupled system on nodal fatigue damage. The proposed approach employs a two-level modelling scheme which combines dynamic analysis for the full train-bridge system and detailed stress analysis at the joint. Miner rule was used to determine the cumulative fatigue damage at critical locations on the welded joint. A sensitivity analysis was conducted for different train loading configurations. It was determined that dynamic vibration negatively influences fatigue life. The calculated cumulative damage at investigated locations can more than the damage estimated using only static moving load method.

Keywords: dynamic effect, dynamic interaction, fatigue damage, railway steel bridge, train-bridge coupled vibration, welded joint.

1. Introduction

With the recent fast development of the railroad infrastructure in China, the number of long span railroad steel bridges has increased significantly. Although, these structures are relatively new, fatigue related performance and safety issues have been a concern during the design process. Fatigue damage (Committee 1982; Fisher 1984) on weld details of some older bridges was discovered in the past and it is recognized as a common structural problem worldwide (Kossakowski 2013). Due to the increased level of train axle loads and repetitive nature of the train loading pattern, fatigue on railroad steel bridges (Fisher, Roy 2011; Zhao *et al.* 1994) has also attracted special attention in structural research (Bowman 1997). Traditionally, fatigue analysis (Bush 1988) of a bridge has been conducted using the method of moving loads and influence line, in which the train axle loads are treated as series of static loads moving along the span of the bridge. The internal force history under moving loads at any given member or connection can be calculated based on the shape of the influence line. These internal force histories will be converted to stress history in order to calculate the cumulative fatigue damage. The impact and dynamic load effects are typically not considered explicitly in a traditional fatigue analysis, but they were included through amplification of stress spectrum using a dynamic impact factor. The value of impact factor depends on a bridge type and it can be referenced from related codes for small span bridges. For large span bridges, special analysis procedures are needed to determine these impact factors. The method of moving load is a quite robust approach, especially, when the dynamic interaction between the vehicle and the bridge is not significant. However, it is likely that such a simplified approach could not capture the actual dynamic load history experienced by bridge structural members.

For steel truss bridges (especially long span cable-stayed or suspended bridges), because the masses of train cars and the bridge girder are comparable, the train-bridge coupled vibration contributes a significant portion of the bridge overall dynamic response. The validity of using a simplified moving load static method for

doi:10.3846/bjrbe.2016.12

bridge joint fatigue evaluation may become questionable. Even though, a simplified dynamic amplification factor can be used, there is currently no widely accepted basis for determination of this factor for long span bridges. Currently, there is a lack of fatigue performance studies on long span railroad bridges considering their true dynamic behaviour. This has provided the impetus for this study.

On the other hand, a significant amount of research (Bhatti *et al*. 1985; Xia, Xu 2000) work was conducted to study the vibration of the train–bridge coupled system. Although these studies do not address fatigue directly, they provided a numerical approach to accurately incorporate dynamic response characteristics (Das *et al*. 2004) of the train–bridge system into fatigue evaluation. This paper is focused on a comparative study between the accumulated damage resulted from traditional static moving load method and a procedure with the train-bridge dynamics fully incorporated. As one of the first attempt to investigate this issue, this study seeks to answer the question that if there is a difference between these two methods and how significant is that difference. Firstly, a train-bridge coupled dynamic analysis program developed by the authors was used to generate time history of the internal force of the members near a critical joint. Then, a detailed FEM (finite element model) for the welded joint was established to study the local stress distribution of the joint given member force time history. The simplified static moving load approach was also conducted parallel to the dynamic study as a comparison. A realistic long span cable-stayed bridge was used as the prototype, also with a series of different train configurations.

2. Case study bridge structure

In order to evaluate the impact of dynamic response on bridge joint fatigue life, a long span cable-stayed steel truss bridge, carrying 2 train lines, has been investigated. The Yujiang bridge (located in Guangxi Province, China), shown in Fig. 1, has a main span of 228 m, designed with double fan cables and two towers. The bridge has a semi-floating support configuration at the main tower and it utilizes triangle steel trusses as the girder. The cross section of the steel truss, which is 15 m wide and 14 m high, is showed in Fig. 1. The truss joints are separated at 12 m (with the joint number illustrated in Fig. 1, which will be used later in this study). All steel members are welded steel plate box sections with maximum plate thickness equal to 44 mm. The dimensions for the top and bottom chords of the truss are shown in Fig. 1 as well.

3. Critical joint by static analysis

Welded truss joint was used for this bridge design due to its high quality from prefabrication and the labour and time savings from straight forward installation on a site. The bridge truss contains many joint components that are welded together and loaded by multiple members from all directions. The stress distribution on these joints is quite complicated. Combined with the potential residual stress levels from welding process, the fatigue performance of such joint structure can be very critical. For the example bridge, there is a total of 80 welded joints (40 on each side). This study will focus on the worst case joint over the length of the bridge based on a static loading analysis.

Since the fatigue behaviour is controlled by stress variation, the joint that experiences the largest stress variation under the moving static vehicle load may be used as the worst case for the entire bridge. In this study, based on the Yujiang Bridge design plan, a CRH2 train car load pattern (Fig. 2) from the Chinese Railway Code (Code for Design of High Speed Railway 2009) was used to perform a static influence line analysis. The analysis was conducted by BANSYS software developed by the Li *et al*. (2005). The analysis only considered the situation of one side loading on a two line bridge (Fig. 2). The envelope for the maximum moments transferred into each welded joint was recorded and presented in Fig. 3.

It can be seen from Fig. 3 that the largest variation of end moment in an influence line analysis occurred at the joints located closest to the bridge towers. On the loading side (where the train load is added, joints A11 and A30 had moment variation close to 300 kNm. The variation

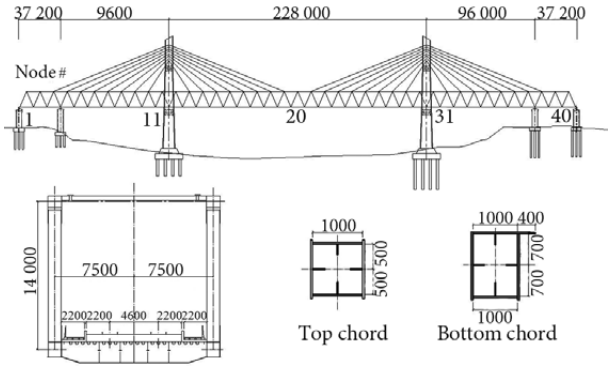

Fig. 1. Example bridge for this study, in mm

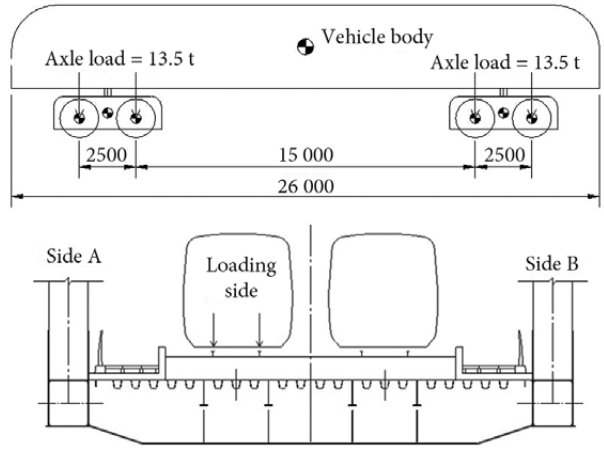

Fig. 2. Train axle pattern and loading locations for the analysis, in mm

on the non-loading side B is less (which is expected), with values at the towers and mid-span varying with a range around 200 kNm. The extreme values of the static moment at these critical locations have been listed in Table 1.

Based on the static analysis, the joint A30 close to the bridge tower was selected as the key joint for detailed fatigue analysis. Although, the dynamic loading response will be different than static loading, it is expected that the load and stresses from these analyses will be strongly correlated. On the other hand, even if the joint A30 is not the absolute worst case joint for fatigue limit state over the entire bridge, the conclusions made based on A30 comparison will still be valid, because the focus of this study is to compare dynamic and static analysis methods relatively.

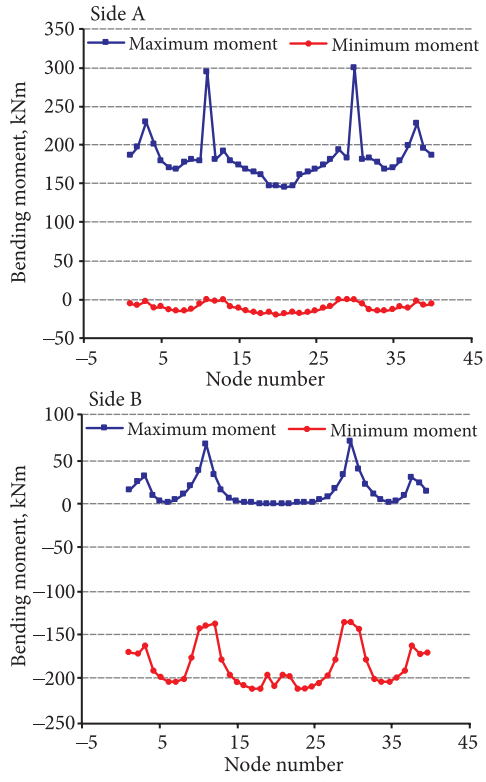

Fig. 3. Max-min moment envelop transferred to each joint under static moving load

Table 1. Maximum and minimum moment transferred to welded joint under static moving load

Joint	Moment, kNm		
	Max	Min	Difference
A11	293.96	0.0036	293.96
A30	299.44	0.0034	299.44
B11	68.04	–140.19	208.23
B20	0.07	–209.83	209.90
B30	72.27	–136.15	208.42

4. Modelling of the train-bridge dynamic effects

In order to incorporate the effect of train-bridge coupled vibration into joint stress analysis, the numerical modelling of this study has been divided into two steps. The first step has utilized a relatively simple bridge model, but it has incorporated the dynamic effects from train-bridge interaction. This step has been based on existing simulation program for train-bridge vibration that has been validated extensively. The second step applies the internal force time history, obtained from the step 1 analysis to a detailed FEM for the welded joint to calculate the stress time history at critical locations. In this study, a static load analysis using moving loads was also performed parallelly to the dynamic time history analysis, with the resulted damage from both methods compared.

4.1. Rail track irregularity

For train-bridge coupled dynamic analysis, besides the moving weight of the train, another main source of excitation is the irregularity of track (Zhai *et al.* 2009). The randomness nature of the track irregularity may have critical impact on internal force of welded joints. Based on previous researches (Zhai *et al.* 2013), the irregularity of the track can be represented as a stationary process and quantified using a power spectrum density function (PSD). Many countries provided recommended PSD for routinely used railway tracks, such as the power spectral density function adopted by Federal Railroad Administration of the U.S., based on rail testing data. The German high speed rail track uneven power spectral density model is the irregularity model adopted by most of European countries currently, which include two levels of irregularity to choose from. In this study, the low level spectrum from Germany was used for the simulation. The rationality for selection of the low level spectrum is to demonstrate the existence of the dynamic effect to fatigue damage under even low level of track irregularity excitation. The spectrum curves for the model were shown in Fig. 4 for horizontal, vertical, and directional irregularity respectively.

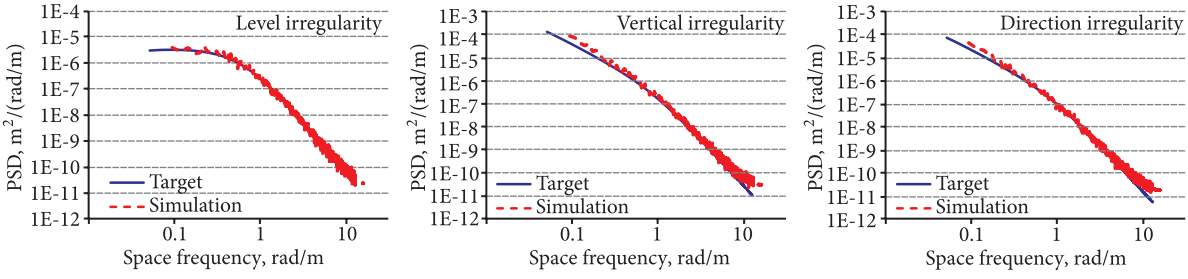

Fig. 4. Power spectrum density function for rail irregularity (German low level spectrum)

4.2. Train-bridge dynamic modelling

Dynamic behaviour of train-bridge coupled system has been a focus in many recent studies from Europe (Diana *et al.* 1989), Japan, and China (Yang *et al.* 1997; Yau *et al.* 2006) due to the rapid growth of high-speed train network in these regions. A viable framework for modelling of train-bridge dynamics has been established. A number of customized simulation software packages were developed by researchers and validated through experimental studies (Shifferaw, Fanous 2013; Wang *et al.* 2014). Most of these programs utilize time history integration of dynamic equations including the train (lumped mass-spring system), the bridge (FEM), and the effect of nonlinear wheel-track interaction (contact and creep relationship). As the focus of this study is not to develop train-bridge models, an existing software package BANSYS (Bridge Analysis SYStem; Li *et al.* 2005) that has been validated in previous studies was used directly. More detailed description of the model and the program were presented in Li *et al.* (2005) for interested readers. The bridge structure was modelled in BANSYS as 3D frame structure, thus it does not directly return the stress time history in the welded joints. Instead, BANSYS model returns the time history of the internal forces in every frame members connected to the welded joint of interest under passing train loads. These internal force time histories were later applied to a detailed FEM for the joint (Fig. 5) to obtain the stress time history. The dynamic force and moment time history calculated from BANSYS for selected members connected to joint A30 were shown in Fig. 6 (member numbering shown in Fig. 5). The corresponding force history calculated using static loads (running the same model with static moving loads) were also plotted and compared. One can see from a force time history comparison perspective, the difference between the two methods may not seem to be significant by visual inspection.

5. Stress analysis of welded joint

In order to obtain the stress time history of the welded joint, a detailed FEM for the joint was established using general FEM program ANSYS. Fig. 5 showed the geometry for a typical joint design and also the FEM rendering from ANSYS for the critical joint. As shown in the figure, this joint was welded together as an integrated piece with legs extended out, and it was connected to all truss members (including the transverse cross beam) using high-strength bolts. The stress distribution on this component can be quite complicated under dynamic loading from all the connected members.

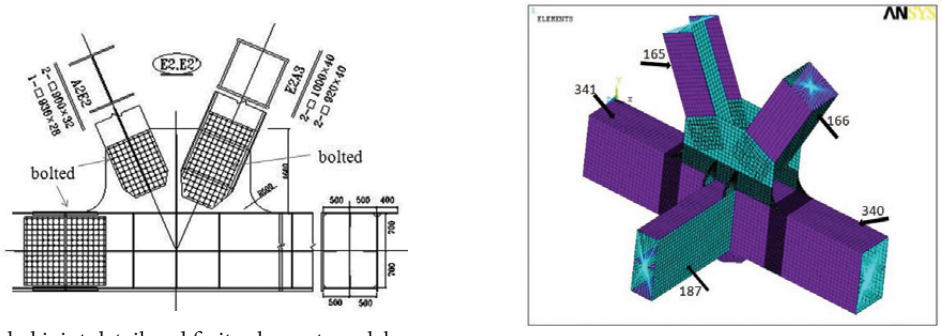

Fig. 5. Critical welded joint detail and finite element model

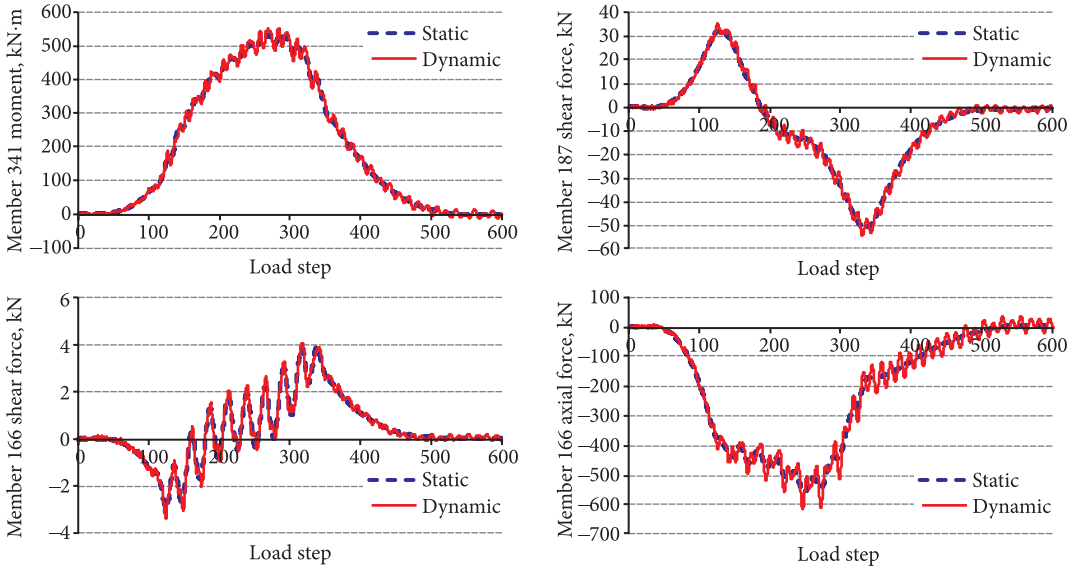

Fig. 6. Internal force time history comparison for selected members

A thin shell element, Shell63, was used to model the joint. Table 2 listed the thickness of the plates used in modelling of the joint. The model was auto-meshed using 100 mm base size elements, except at the joint area where a smaller grid at 20 mm was used, the model was divided into a total of 600 572 nodes and 13 695 elements. The members leading into the node were modelled including 1/3 of their total length in order to eliminate localized effects on the stresses. At the end of each member, MPC184 rigid body element was used to establish a rigid zone in order to apply the simulated dynamic internal force loading history from BANSYS. The static load history from moving load analysis was also applied to this model.

Table 2. Plate thickness for the welded joint

Gusset plate	Bottom chord flange	Bottom chord web	Stiffeners	Lateral beam	Cross member flange	Cross member web
mm						
24	20	24	20	32	32	28

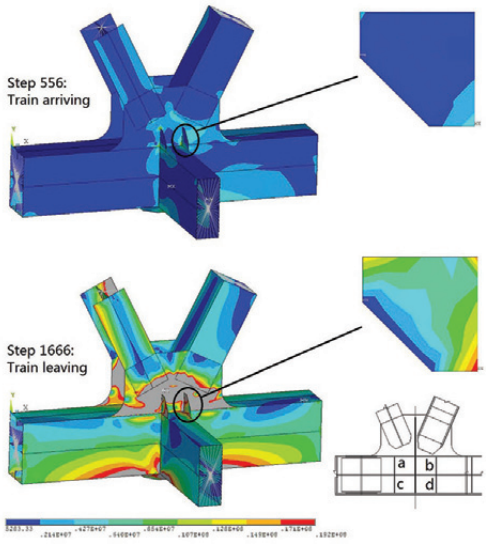

Fig. 7. Simulated stress time history based on static and dynamic loading, in Pa

Although the time history of the internal forces in all the connected members applied to the detailed ANSYS model are in self-equilibrium, the joint model still needs to be restrained in order to ensure numerical stability during the analysis and avoid rigid body movement. Based on past research experience, a set of simple boundary condition was added to the model, so the system is statically determinate and stable.

5.1. Stress analysis

Through the detailed joint model and the variation of stresses over time can be captured. Based on the stress distribution characteristics and revealed by the FEM model, the intersection points between the lateral beam and the welded joint have a relatively large stress concentration. At the corners of the connection, the joint is strengthened by stiffener plates which also experience high level of stress variation. Fig. 7 has showed an illustrative example of the change in stress on a stiffener plate within the welded joint from the dynamic analysis. In Fig. 8 one can see that there is the significant change in Von Mises stress distribution between the time step, when the train just arrived at the joint (step 556), and when the entire train left the joint (step 1666). Based on the stress distributions on various parts of the welded joint, it was discovered that there is stress concentration at the corners of the joint plate and gusset plate. These locations will likely represent the worst case locations within the joint for cumulative fatigue damage. Thus, the current example will focus on assessing fatigue damage accumulation at these 4 points, marked a, b, c, and d at the corners of the beam-truss intersection. The time history

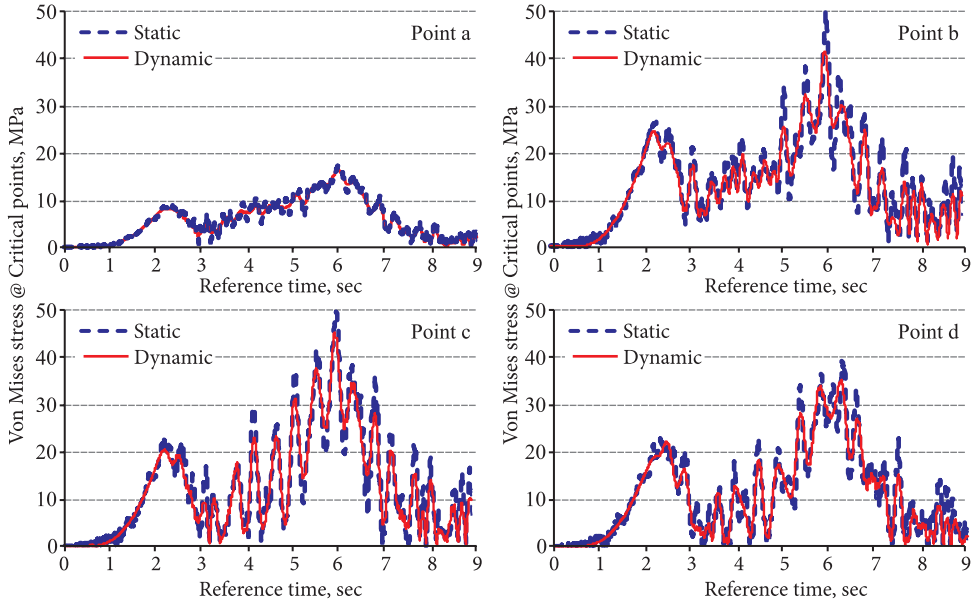

Fig. 8. Stress time history for critical locations

of Von Mises stresses under passing of one standard train with eight cars was plotted in Fig. 8 for these critical locations. Similarly, the corresponding static load analysis results were also shown in the figure for comparison.

Similar to the member internal force comparison, the comparison between the dynamic and static stresses reveals that the dynamic effect seems to be not significant if only the maximum stress level is of concern. There are variations of stress distribution over different locations on the welded joint. The results of dynamic analysis have more cycles of stress variation at all examined locations than static force analysis. Note that the stress, induced by the bridge dead load, has been eliminated from the plots. The maximum stress happens at close to 2 second and 6 second time stamp, because these are the time point when the train head arrives and train tail leaves the joint location.

5.2. Fatigue damage analysis

In order to obtain the fatigue damage accumulation resulted from the passing train, classical rain-flow counting method was used to obtain the stress spectrum based on the stress time history. Firstly, the Miner linear damage accumulation theory was used to convert variation stress cycles to constant stress cycles. Then, the stress variation amplitude was recorded and counted into different bins with 2 MPa increments. The number of stress cycles that fall within the range were counted and plotted, resulting in a discrete stress variation count shown in Fig. 9 for all critical locations (the number on top of the bar plot indicates the total number of cycles). Note that both the dynamic and static time histories were processed in the same way and compared side-by-side.

It can be seen from Fig. 9 that stress variation for dynamic cases was constantly higher than that from static analysis, which is expected. A more direct comparison of the dynamic and static cases can be conducted through calculation of the cumulative fatigue damage based on Palmgren-Miner rule. Since the objective of this comparative study is to identify the difference of the dynamic and static calculation, a relatively simple fatigue damage calculation formulation based on *BS5400: Steel, Concrete and Composite Bridges – Part 10: Code of Practice for Fatigue* was adopted. A threshold fatigue failure stress limit (σ_0) was set to 36 MPa. Based on the traffic condition of the bridge in this study, the annual total train traffic is estimated to be 3484 times/year. The cumulative fatigue damage calculation based on BS5400 is:

$$D = \sum \frac{n}{N} = \left(\frac{n_1}{N_1} + \frac{n_2}{N_2} + \cdots + \frac{n_n}{N_n} \right), \quad (1)$$

and for various stress cycle levels:

$$\sigma_r \geq \sigma_0, \ \frac{n}{N} = \frac{n\sigma_r^m}{K_2} = \frac{n}{10^7} \left(\frac{\sigma_r}{\sigma_0} \right)^m, \quad (2)$$

$$\sigma_r \leq \sigma_0, \ \frac{n}{N} = \frac{n\sigma_r^{m+2}}{K_2\sigma_0^{m+2}} = \frac{n}{10^7} \left(\frac{\sigma_r}{\sigma_0} \right)^m, \quad (3)$$

where n_1, n_2, …, n_n – the total number of repetition of stress cycle with amplitudes σ_1, σ_2, …, σ_n during the design life of the structure; N_1, N_2, …, N_n – the fatigue life of the detail under constant stress cycles with amplitudes σ_1, σ_2, …, σ_n; σ_0 – constant amplitude non-propagating stress range; σ_r – Range of stress (stress range) in any one cycle; K_2 - parameter defining the σ_r – N relationship for two standard deviations below the mean line; m – inverse slope of $\log\sigma_r$ – $\log N$ curve, in this study $m = 3$.

Based on the discrete stress counts, one can calculate the cumulative damage at the corner points under one

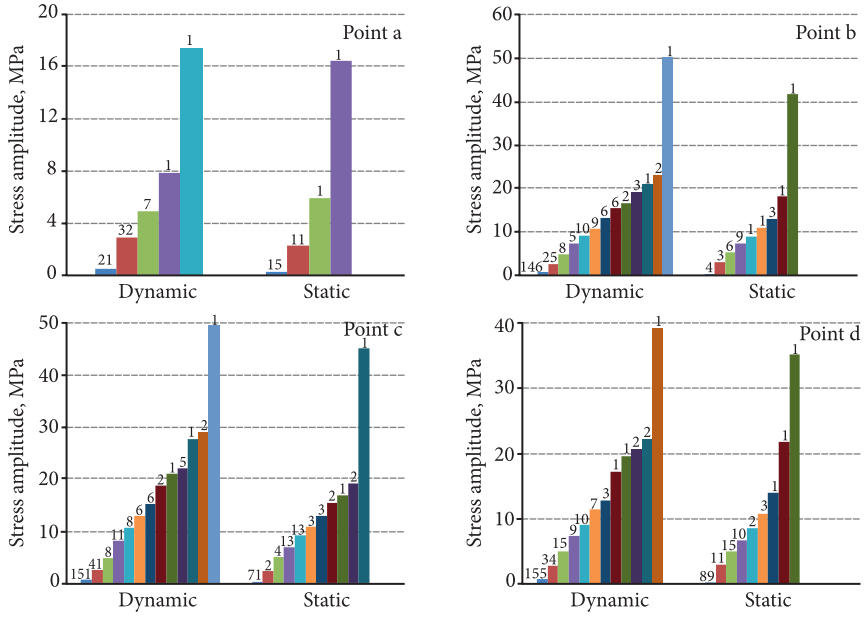

Fig. 9. Discrete stress variation counts at critical points under one train pass

Table 3. Cumulative damage at critical points

Critical points	Damage under one train pass D'		Life cycle cumulative damage D		Dynamic/Static
	Static	Dynamic	Static	Dynamic	
a	1.76E-09	2.36E-09	6.13E-04	8.22E-04	134%
b	1.52E-07	2.99E-07	5.29E-02	1.04E-01	196%
c	1.96E-07	3.84E-07	6.83E-02	1.33E-01	195%
d	8.16E-08	1.56E-07	2.84E-02	5.64E-02	198%

train passing and during the total design life (100 Years) using Eqs (2)–(3). The results were shown in Table 3.

From the results in Table 3, the cumulative damage at all corner points in the example bridge structure is quite small (far less than 1.0 over the life of the bridge). Thus the design of the welded joint is satisfactory against fatigue failure, which is expected, because this is a realistic

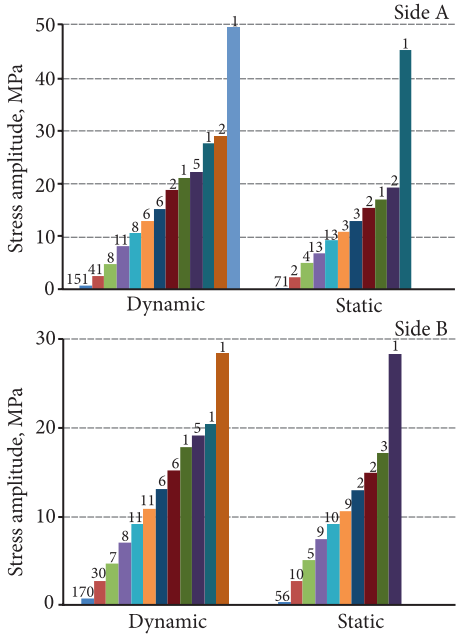

Fig. 10. Discrete stress variation counts at point C under different line load

Table 4. Cumulative damage at point C under different line load

Line load	Life cycle cumulative damage D		Dynamic/ Static
	Static	Dynamic	
Side A	6.83E-02	1.33E-01	195%
Side B	1.35E-02	2.32E-02	172%

Table 5. Different train car arrangements considered

Case	Speed, km/h	Car arrangement
1	200	1 motor
2	200	2×(1 trailer + 1 motor + 1 motor + 1 trailer)
3	200	4×(1 trailer + 1 motor + 1 motor + 1 trailer)

bridge designed for train loading even higher than CRH2 type used in this analysis. Based on the damage index, the point C represents the worst case scenario for fatigue and it will be the focus of sensitivity study later on. One of the most significant observations from this analysis is the difference between the damage calculated using traditional static method and the coupled dynamic model. The dynamic analysis always produces larger damage accumulation. Among the critical points, considered in this study, the cumulative damage calculated considering dynamic response is nearly double the damage estimated using static method. This reveals a potential need for the inclusion of train-bridge coupled analysis for fatigue evaluation of railroad long span steel bridges. Although the absolute maximum stress values were only slightly affected by the dynamic vibration, added number of cycles and increased stress variation led to significant difference in fatigue life expectance.

6. Sensitivity analysis of loading conditions

In order to evaluate the consistency of this observed difference between the fatigue damage prediction using static load and dynamic simulation, several different loading conditions were investigated in this study. Firstly, the same train configuration was applied to different railway track lines. The train configuration used was 2 sets (1 trailer + 1 motor + 1 motor + 1 trailer), added to each of the train lines (side A and B) separately with the speed of 200 km/h. The resulted stress spectrum from the truss joints at loading and empty sides were both shown in Fig. 10 for point C (on side A), together with the calculated cumulative damage in Table 4.

The results in Table 4 indicated that the change in train configuration and loading location affected the fatigue damage in the joint. When the train load was applied to the side further away from the joint of interest, the damage is significantly smaller, which is simply expected from structural analysis. However, the dynamic approach consistently produces about twice as much damage as the static load estimation.

In order to further investigate the sensitivity of fatigue damage calculation to train configuration, additional 3 sets of train car arrangements were analysed, as it is shown in Table 5. All trains are loaded at the side of the critical point C.

Again, the analysis was conducted using both, static and dynamic approaches, with a focus on damage accumulation at point C. The resulted stress spectrum

and cumulative damage were listed in Fig. 11 and Table 6 respectively. It is seen that the fatigue damage will increase when the number of train cars increases. The distinct difference between the dynamic and static approaches still exists, with dynamic estimation more than double the static prediction in some cases.

7. Conclusions

In order to evaluate the impact of dynamic train-bridge interaction on the fatigue life of railroad steel bridges, a detailed numerical study was conducted to compare the accumulative damage on critical welded joint of a two line cable-stayed bridge. The fatigue damage was calculated using two different methods, namely, the traditional static moving load method and nonlinear train-bridge coupled dynamic simulation. Some interesting conclusions are obtained through this study, including:

1. For steel truss cable-stayed bridges similar to the example used here, the worst joint for fatigue analysis is likely to locate close to the main towers. If welded joint detail was used, severe stress concentration may occur at the location where the transverse beam is welded in to the joint.

2. For typical traffic condition represented by the example structure, the cumulative fatigue damage is not high over the bridge life span, no matter which estimation method is used. The current design for the example bridge is satisfactory with regard to fatigue under train loads.

3. The fatigue damage estimated using full dynamic simulation is significantly greater than the value estimated using traditional static moving load method. This difference was consistently observed for several different loading conditions examined in this study. When the design of a railway bridge structure is controlled by fatigue, it is critical to include the effect of train-bridge dynamic interaction or use the appropriate dynamic amplification factors. Otherwise, the design may not be conservative.

4. The fatigue damage for a given location increases with the number of train cars included. The traffic volume on a railway bridge is another critical design factor for its fatigue life.

5. It needs to be noted that this study only looked into one example bridge configuration. It is likely that for any long span bridges where the train-bridge coupled vibration response is significant, similar conclusions can be made. However, analysis including more bridge types and configurations should be studied in the future to further validate the findings from this study.

Acknowledgements

The writers are grateful for the financial supports from the National Natural Science Foundation of China under Grant NNSF–51525804, U1334201, the Sichuan Province Youth Science and Technology Innovation Team(2015TD0004) and the National Key Basic Research Development Plan of China (2013CB036206).

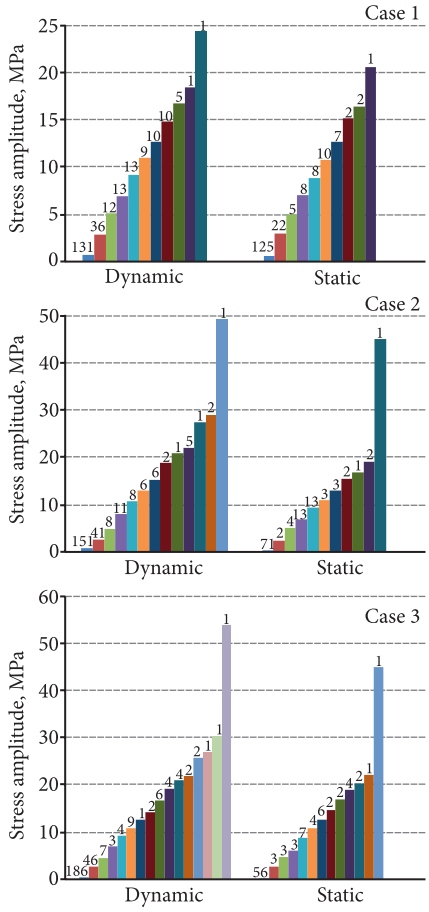

Fig. 11. Discrete stress variation counts at point C under different train load

Table 6. Cumulative damage at point C under different train load

Case	Life cycle cumulative damage D		Dynamic/Static
	Static	Dynamic	
1	6.23E-03	1.54E-02	247%
2	6.83E-02	1.33E-01	195%
3	7.87E-02	1.65E-01	210%

References

Bhatti, M. H.; Garg, V. K.; Chu, K. H. 1985. Dynamic Interaction Between Freight Train and Steel Bridge, *Journal of Dynamic Systems Measurement and Control–Transactions of the ASME* 107(1): 60–66. http://dx.doi.org/10.1115/1.3140708

Bush, A. 1988. *Fatigue Strength Calculation*. Switzerland: Trans Tech Publications. 467 p.

Bowman, M. D. 1997. Fatigue Design and Retrofit of Steel Bridge, *Structural Engineering and Materials* 1(1): 107–114. http://dx.doi.org/10.1002/pse.2260010116

Committee, A. 1982. Fatigue and Fracture Reliability of the Structural Safety and Reliability, *Journal of the Structural Division* 108(1): 83–88.

Diana, G.; Cheli, F. 1989. Dynamic Interaction of Railway Systems with Large Bridges, *Vehicle System Dynamics* 18(1–3): 71–106. http://dx.doi.org/10.1080/00423118908968915

Das, A.; Dutta, A.; Talukdar, S. 2004. Efficient Dynamic Analysis of Cable-Stayed Bridges Under Vehicular Movement Using Space and Time Adaptivity, *Finite Element in Analysis and Design* 40(4): 407–424. http://dx.doi.org/10.1016/S0168-874X(03)00070-2

Fisher, J. W.; Roy, S. 2011. Fatigue of Steel Bridge Infrastructure, *Structure and Infrastructure Engineering* 7(7–8): 457–475. http://dx.doi.org/10.1080/15732479.2010.493304

Fisher, J. W. 1984. *Fatigue and Fracture in Steel Bridges*. New York: John Wiley & Sons. 315 p.

Kossakowski, P. G. 2013. Fatigue Strength of an over One Hundred Year Old Railway Bridge, *The Baltic Journal of Road and Bridge Engineering* 8(3): 166–173. http://dx.doi.org/10.3846/bjrbe.2013.21

Li, Y. L.; Qiang, S. Z.; Liao, H. L.; Xu, Y. L. 2005. Dynamics of Wind–Rail Vehicle–Bridge Systems, *Journal of Wind Engineering and Industrial Aerodynamics* 93(6): 483–507. http://dx.doi.org/10.1016/j.jweia.2005.04.001

Shifferaw, Y.; Fanous, F. S. 2013. Field Testing and Finite Element Analysis of Steel Bridge Retrofits for Distortion-Induced Fatigue, *Engineering Structures* 49: 385–395. http://dx.doi.org/10.1016/j.engstruct.2012.11.023

Wang, H.; Xia, H.; Zhan, J. W. 2014. Modeling and Dynamic Characteristics Analysis of the Qiantangjiang Rail-Cum-Road Bridge, *Applied Mechanics and Materials* 501–504: 1187–1193. http://dx.doi.org/10.4028/www.scientific.net/AMM.501-504.1187

Xia, H.; Xu, Y. L. 2000. Dynamic Interaction of Long Suspension Bridges with Running Trains, *Journal of Sound and Vibration* 237(2): 263–280. http://dx.doi.org/10.1006/jsvi.2000.3027

Yang, Y. B.; Yau, J. D.; Hsu, L. C. 1997. Vibration of Simple Beams Due to Trains Moving at High Speeds, *Engineering Structures* 19(11): 936–944. http://dx.doi.org/10.1016/S0141-0296(97)00001-1

Yau, J. D.; Yang, Y. B. 2006. Vertical Accelerations of Simple Beams Due to Successive Loads Traveling at Resonant Speeds, *Journal of Sound and Vibration* 289(1–2): 210–288. http://dx.doi.org/10.1016/j.jsv.2005.02.037

Zhao, Z. W.; Haldar, A.; Breen, F. L. 1994. Fatigue-Reliability Evaluation of Steel Bridges, *Journal of Structural Engineering* 120(5): 1608–1623. http://dx.doi.org/10.1061/(ASCE)0733-9445(1994)120:5(1608)

Zhai, W. M.; Xia, H.; Cai, C. B.; Gao, M.; Li, X.; Guo, X.; Zhang, N.; Wang, K. 2013. High-Speed Train-Track-Bridge Dynamic Interactions – Part I: Theoretical Model and Numerical Simulation, *International Journal of Rail Transportation* 1(1–2): 3–24. http://dx.doi.org/10.1080/23248378.2013.791498

Zhai, W. M.; Wang K. Y., Cai, C. B. 2009. Fundamentals of Vehicle-Track Coupled Dynamics, *Vehicle System Dynamics* 47(11): 1349–1376. http://dx.doi.org/10.1080/00423110802621561

Received 24 March 2015; accepted 13 May 2015